Int J Adv Manuf Technol (2017) 91:2383–2400
DOI 10.1007/s00170-016-9929-x

ORIGINAL ARTICLE

An improved cutting power model of machine tools in milling process

Lirong Zhou[1] · **Jianfeng Li**[1] · **Fangyi Li**[1] · **Xingshuo Xu**[1] · **Liming Wang**[1] · **Geng Wang**[1] · **Lin Kong**[1]

Received: 18 May 2016 / Accepted: 18 December 2016 / Published online: 4 January 2017

Abstract Establishing a rapid, accurate, and practical energy consumption evaluation model for machine tools is essential to save energy and increase profits in the manufacturing industry. Relationships between spindle rotation speed, cutting parameters, material removal rate, specific energy consumption, cutting power, and material removal power were experimentally analyzed, and the limitation and the limitation and differences between several machine tools' cutting power evaluation models were discussed. Cutting parameters or material removal rate were regarded as independent variable in those models. By comparing the models' fitting and predicted results, it draw a conclusion that the model treating cutting parameters as independent variable had greater accuracy but depends on a large quantity of experimental data. The model treating material removal rate as independent variable can also obtain a good fit and reduce the number of necessary experiments. Therefore, it is a rapid method to estimate the cutting energy consumption of machine tools for the latter model. In addition, the paper puts forward an improved cutting power model, which considers the influence of the spindle rotation speed on the material removal power during the milling process. The proposed model can predict a milling machine's cutting power more accurately.

Keywords Machine tools · Energy consumption model · Cutting power · Green manufacturing

✉ Jianfeng Li
jianfeng_li1@163.com

[1] School of Mechanical Engineering, Shandong University, Jingshi Road, No. 17923, Jinan, Shandong 250061, China

Abbreviation

a_p	Cutting depth (mm)
a_s	Cutting width (mm)
d	Workpiece diameter (mm)
D	Cutting tool diameter (mm)
E	The total energy consumption of the machine tool (kWh)
E_{cut}	Cutting energy consumption (kWh)
f_z	Feed per tooth (mm)
f	Feed per revolution (mm/r)
F	Cutting force (N)
H	Brinell hardness (N/mm^2)
MRR	Material removal rate (mm^3/s)
n	Spindle rotation speed (r/min)
P_{in}	Machine tool input power (kW)
P_{cut}	Machine tool input power in cutting (kW)
P_{idle}	Machine tool input power in no load (kW)
$P_{material}$	Material removal power (kW)
$P_{spindle}$	Spindle power (kW)
$P_{standby}$	Machine tool standby power (kW)
$P_{auxiliary}$	Machine tool auxiliary equipment power (kW)
P_{feed}	Feed shaft power (kW)
SEC	Specific energy consumption (J/mm^3)
t_a	The spindle acceleration time (ms)
v_c	Cutting speed (mm/min)
v_f	Feed speed (mm/min)
$V_{material}$	Material removal volume (mm^3)
$\overline{VB}$	Average flank wear width of cutting tool (mm)
z	The number of teeth on the cutting tool
β	Normal friction angle (rad)
γ	Cutting tool rake angle (rad)
η_s	Shear flow angle (rad)
λ	Oblique angle (rad)
φ	Shear plane angle (rad)
φ_{in}	Angle of a cutting tooth entering a cutting zone (rad)

ψ	Immersion angle (rad)
τ	Workpiece flow stress (Pa)
μ	Coefficient of sliding friction between a workpiece and cutting tool

1 Introduction

With the development of human society, contradictions between economic development and environmental constraints have become more apparent. Manufacturing is the main creator of jobs and wealth and also the source of many environmental problems. It is necessary to create sustainable manufacturing solutions that reduce costs, resource consumption, energy consumption, and environmental emissions [1]. The US Energy Information Administration (EIA) energy statistics yearbook pointed out that in 2013, its industrial sector energy consumption accounted for 34% and carbon dioxide emissions associated with industrial energy accounted for 27.5% of the country's total emissions. In addition, carbon dioxide emissions in manufacturing accounted for 81.7% out of the entire industrial field [2]. According to the data from China's national bureau of statistics, the manufacturing energy consumption accounted for 57.3% of its total energy consumption in 2013 [3], and it was said that the emissions of environmental pollution caused about 70% from the manufacturing [4]. In addition to environmental concerns, the EIA indicated that from 2013 to 2040, the retail prices of industrial electricity and oil are expected to rise at an average annual growth rate of 0.7% in the USA [2].

Global warming, growth of demand for energy, and rising energy prices have required the manufacturers to look for high-energy efficiency and low-cost manufacturing plans, and academic circles have begun to pay more attention to energy consumption models and energy efficiency research with regard to manufacturing [5, 6]. Machining process industry is an important part of manufacturing, in which machine tools are widely used [7]. The environmental impact of machine tools is mainly due to consuming large amounts of electric energy and indirectly generating carbon dioxide emissions [8]. An accurate energy consumption evaluation model is useful for companies to build energy labels for machine tool products or associated products. The standard ISO14955-1 for machine tools focuses on using phase of energy supply and consumption to carry out environmental impact assessment and energy-saving design. However, the international standard on metal cutting and metal forming machine tool energy efficiency test specification is still being written [9]. Assessing machining process energy consumption accurately and quickly can provide a basis for judging and decision-making guidance in energy-saving machine tool design and process planning, which is the premise of improving the energy efficiency of machining systems [10, 11]. Therefore, establishing rapid, accurate, and practical energy consumption evaluation models for machine tools under various machining conditions is very important for saving energy in the manufacturing industry [12].

The key to evaluate the energy consumption of a machine tool is to understand the power characteristics of its components. The power or energy consumption characteristics not only depend on its performance of internal composition system and running state changes but also on the object being processed and processing conditions. Domestic and foreign scholars have put forward different machine tool power or energy consumption evaluation models [5]. Liu et al. [13] established an energy consumption model of a machine tool's main transmission system, which included running states such as cutting, no load, and start. The related equations are:

$$E = \int_0^{t_1} P_{\text{in}}(t)\mathrm{d}t + P_{0t_2} + \left(P_{0t_3} + \int_0^{t_3} P_a(P_{\text{cut}}(t))\mathrm{d}t + \int_0^{t_3} P_{\text{cut}}(t)\mathrm{d}t\right) \quad (1)$$

$$P_a = \alpha_1 P_{\text{cut}}(t) + \alpha_2 P_{\text{cut}}(t)^2 \quad (2)$$

Where t_1~t_3 represents time of start, no load, and cutting. P_{in} is input power of the main transmission system. P_0 is idle power. P_a is the mechanical and electrical load loss power, and it was the function of the cutting power (P_{cut}), a_1 and a_2 were additional load loss coefficients obtained by fitting.

Lv et al. [14] regarded energy consumption units as movement elements of the machine tool, establishing a power model of turning machine. Their equations were:

$$P = P_{\text{SO}} + P_{\text{L}} + P_{\text{CC}} + P_{\text{CFS}} + P_{\text{spindle}} + \left(P_x + P_y + P_z\right) + P_{\text{TS}} + P_{\text{TC}} + P_{\text{cut}} \quad (3)$$

$$P_{\text{cut}} = (1+\alpha)F_{v_c} \quad (4)$$

Where P_{SO}, P_{CFS}, P_{CC}, P_{L}, P_{TS}, and P_{TC} represented power related to the basic module, cooling device, chip removal device, lighting device, tool choose and tool change device respectively. P_{spindle}, P_x, P_y, and P_z were spindle power and feed power in x/y/z directions, respectively. F_{v_c} was theoretical cutting power. a was an additional load loss coefficient due to cutting power. The calculation of cutting power in literature depends on the acquisition of additional load loss coefficients [13, 14]. Collecting such coefficients requires a large number of experiments, and the rapid acquisition of such data remains an area for further study.

Zhong et al. [15] pointed out that a material removal power of turning machine can be transformed into the power caused by cutting force, as shown in Eq. (5).

$$P_{\text{material}} = F_{v_c} = \left(c_1 \times {a_p}^{c_2} {f^{c_3}}_{v_c}{}^{c_4} \times k\right)_{v_c}. \quad (5)$$

Where material removal power (P_{material}) was the material removal power, the power at the tip of the cutting tool, F was

the cutting force, v_c was the cutting speed, a_p was the cutting depth, f was the feed per revolution, c_1 was the correlation coefficient determined by workpiece and cutting condition, k was an associated factor, and c_2~c_4 represented corresponding indexes, whose values were determined by empirical research.

Munoz et al. [16] established a cutting energy model based on the plastic deformation force of metal and material removal velocity vector, as shown in Eq. (6).

$$E_{\text{cut}} = \left(\frac{\cos(\beta-\gamma)\cos\eta_s\cos\lambda + \cos(\varphi+\beta-\gamma)\sin\eta_s\sin\lambda}{\cos(\varphi+\beta-\gamma)}\right)\frac{\tau \times V_{\text{material}}}{\sin\varphi\cos\lambda} \tag{6}$$

Where β was normal friction angle, γ was the cutting tool rake angle, η_s was the cutting flow angle, φ was shear plane angle, τ was plastic flow stress of the work piece, λ was the inclination angle, and V_{material} was material removal volume.

Kishawy et al. [17] established a cutting energy model E_{cut}, which included plastic deformation energy of primary and shear zones, and metallic particles energy of stripping. The calculation model contained the strain hardening index, shear angle, cut chip friction force, cutting chip thickness ratio, Poisson's ratio for the material, Young's modulus, fracture stress, and crack length parameters. The latter two cutting energy models in literature are complex, and the accuracy can be improved.

Shao et al. [18] established a cutting power model such as Eq. (7), which considered the cutting tool parameters, cutting tool wear, and cutting parameters.

$$P_{\text{cut}} = \text{znDa}_p\left\{Kh^{-c}f_z(\cos\varphi\text{in}-\cos(\varphi\text{in}+\psi)) + \mu H\overline{\text{VB}}\psi\right\}\Big/2 \tag{7}$$

Where z was number of cutter teeth, D was cutting tool diameter, c was the chip thickness constant, f_z was feed per tooth, H was the workpiece Brinell hardness, K was the cutting force constant, $\overline{\text{VB}}$ was average flank wear width of the cutting tool,μ was the coefficient of sliding friction between a workpiece and cutting tool, φ_{in} was angle of a cutting tooth entering a cutting zone, and Ψ was the immersion angle.

Yoon et al. [19] pointed out that there was a linear relationship between cutting power and the amount of tool wear $\overline{\text{VB}}$. It is difficult to measure the consistency between cutting parameters and cutting tool life, so the model based on tool wear has some difficulties calculating the energy consumption of the machining process.

Although the performance of machine tools, workpiece materials, cutting tool, and cutting parameters will cause a change in a machine tool's power, it is difficult to develop a machine tool energy consumption model taking all factors into account, because it requires a large amount of experimental data to train and fit the predicting model for a given process.

The cutting power of a machine tool is mainly affected by cutting parameters. Therefore, in order to quickly estimate the energy consumption of a machine tool during a cutting process, an important concept has been developed, namely the specific energy consumption (SEC). SEC is defined as the energy required to remove materials of a unit volume or quality. SEC can be expressed as:

$$\text{SEC} = \frac{E}{V_{\text{material}}} \quad \text{or} \quad \text{SEC} = \frac{P_{\text{cut}}}{\text{MRR}} \tag{8}$$

Where the material removal rate (MRR) is a function of cutting parameters. SEC covers the mapping relationship between MRR and cutting energy consumption. Although the existing models of SEC are not accurate, SEC has been widely used because it is easy to ascertain the model coefficients.

The following studies put forward similar SEC models for machine tools. Gutowski et al. [20] divided machine tool power into idle power and material removal power during the cutting process:

$$P_{\text{cut}} = P_{\text{idle}} + k \times \text{MRR} \tag{9}$$

where P_{idle} is idle power and $k \times$ MRR represents the power required remove material. Gutowski's research pointed out that the constant k(kJ/cm^3) depended on the physical characteristics, which were related to workpiece material and the cutting tool. Diaz et al. [22] obtained an inverse ratio curve relationship between the SEC and the MRR by changing cutting depth and cutting width. Literatures such as [20–22] put forward of similar SEC models of machine tools, like as:

$$\text{SEC} = c_1 + \frac{c_2}{\text{MRR}} \tag{10}$$

Actually, the Eq. (10) is a variable form of the Eq. (9) divided by the MRR on both ends. Where c_1~c_2 are fitting coefficients.

Li et al. [23] considered P_{idle} to consist of standby power (P_{standby}) and spindle power (P_{spindle}). P_{spindle} is a linear function of the spindle rotation speed n:

$$P_{\text{spindle}} = a \times n + b \tag{11}$$

Li et al. [23] also put forward cutting power and SEC of a milling machine as:

$$P_{\text{cut}} = P_{\text{standby}} + a \times n + b + k \times \text{MRR} \tag{12}$$

and

$$\text{SEC} = c_1 + \frac{c_2 \times n}{\text{MRR}} + \frac{c_3}{\text{MRR}} \tag{13}$$

Where c_1~c_3 were fitting coefficients. They additionally discussed the meaning of coefficients and pointed out that b was power loss caused by the motor and transmission chain of the main drive system. a and k were coefficients affected by the inherent properties of a given machine tool and workpiece

materials. Their model showed an improved accuracy due to disassembling P_{idle} and taking n into account as part of their in SEC evaluation in the milling process.

Guo et al. [24] pointed out that the SEC of a turning machine was not only related to the cutting parameters but also related to the workpiece diameter d, because cutting speed v_c of turning was related to n and d. Their SEC model of a turning process was:

$$\mathrm{SEC} = \frac{c_1}{v_c \times v_f \times a_p} + c_2 \times {v_c}^{c_4} \times {v_f}^{c_5} \times ap^{c_6} \times d^{c_7}. \quad (14)$$

Where c_1~c_7 were fitting coefficients.

The SEC model of a machine tool can be acquired by using a three-factor three-level orthogonal experiment after a specific cutting tool and material are given. The coefficients in the SEC model can be quickly determined with less experimental data required, which increases the convenience of estimating a machine tool's energy consumption during the cutting process [25]. The main arguments surrounding SEC models in literature [20–23] is that they consider the same MRR, which leads to the same SEC and P_{cut}. Jia et al. [26] pointed out that when using different combinations of cutting parameters to get the same MRR, the actual measured cutting power is not the same. However, there is still a lack of research that discusses the differences between these models with regard to MRR or cutting parameters as an independent variable in detail. Establishing an accurate cutting power model is the foundation of evaluation and optimization of the machine tool's energy consumption. The accuracy of existing models remains to be further increased. Firstly, this paper analyzed the relationships between spindle rotation speed (n), cutting parameters, MRR, SEC, P_{cut}, and $P_{material}$. Then, this paper discussed the differences between models regarding MRR or cutting parameter as independent variable to predict cutting power. Finally, this paper puts forward an improved cutting power model for a milling process that considers the influence of the spindle rotation speed on material removal power. The improved model is proved to increase prediction accuracy of milling machine cutting power.

2 The machine tool energy consumption model and hypothesis

2.1 The introduction of basic model

An energy consumption model usually refers to the power model. Machine tool energy consumption status generally includes starting state, acceleration state, deceleration state, standby state, air-cutting state, cutting state, and auxiliary status. This paper does not make discussion on power of starting, acceleration, and deceleration states due to its short time.

(1) Standby power: power required to remain stable after a machine has powered up. It is used to maintain the normal operation of the power components of a machine tool such as the numerical control system, fan, display, and lubrication system. These components generally remain open after the machine starts and will not shut down unless the machine is turned off. Usually, the standby power can be expressed as:

$$P_{standby} = P_{fan} + P_{control-panel} + P_{screen} + P_{lubrication} \quad (15)$$

(2) Idle power: refers to the input power of the machine tool when the spindle and feed axis have already begun to move, but the cutting tool has not contacted with the workpiece. Some studies also call it air-cutting power, meaning power under no load. P_{idle} contains instantaneous $P_{standby}$, $P_{spindle}$, and feed power (P_{feed}), as shown in Eq. (16).

$$P_{idle} = P_{standby} + P_{spindle} + P_{feed} \quad (16)$$

The power of the spindle is a linear function of spindle rotation speed, n (r/min), when idling at a constant speed, as shown in Eq. (17).

$$P_{spindle}(n) = a \times n + b \quad (17)$$

Where a and b are fitting coefficients that relate to the spindle motor power loss and the friction loss [26]. The power of X/Y/Z feed shaft is a linear function of feed speed v_f, as shown in Eq. (18), Where a' and b' are also fitting coefficients. In general, P_{feed} is a very small proportion of overall input power of the machine, so it can be seen as constant C or neglected [23].

$$P_{feed}(v_f) = a' + b' \times v_f \approx C \quad (18)$$

(3) Cutting power: the total input power of the machine tool when materials are cut. This section contains the $P_{standby}$, $P_{spindle}$ (n), P_{feed} (v_f), and $P_{material}$, as shown in Eqs. (19) and (20). Gutowski et al. [20] think that the cutting power of machine tool includes constant power and variable material removal power, as Eq. (9). Li et al. [23] improves it on the basis of Gutowski et al.'s [20] research, as shown in Eq. (12), and he thinks that P_{cut} includes the standby power, air-cutting power, and material removal power. Because the feed shaft power is small, it is

ignored in Li's research. Equation (20) is reasoned out with the models of Gutowski et al. [20] and Li et al. [23].

$$P_{\text{cut}} = P_{\text{standby}} + P_{\text{spindle}}(n) + P_{\text{feed}}(v_f) + P_{\text{material}} \tag{19}$$

$$P_{\text{material}} = k \times \text{MRR} \tag{20}$$

The previous three parts of Eq. (19) are mainly affected by machine tool automation, energy transfer efficiency of the mechanical system, electric energy, and hydraulic system conversion efficiency, which embody the inherent energy consumption characteristics of the machine tools. P_{material} refers to the additional power needed when machine tools are cutting material, and k is the coefficient related to the physical characteristics in the machining process. P_{material} is closely related to the material removal rate and cutting conditions. For the milling process:

$$\text{MRR}\left(\text{mm}^3/\text{s}\right) = \frac{v_f \times a_p \times a_e}{60} \tag{21}$$

Where v_f is the feed speed of milling cutter relative to the workpiece, a_p is cutting depth, and a_e is cutting width [23]. For the turning process:

$$\text{MRR}\left(\text{mm}^3/\text{s}\right) = \frac{v_c \times f \times a_p}{60} \tag{22}$$

Where v_c is cutting speed and f is feed per revolution [14].

(4) Auxiliary power: the power generated when auxiliary function components of a machine tool selectively open during the machining process. Auxiliary function components include lighting device, cooling liquid device, chip removal device, tool change device, etc. Auxiliary power calculation is shown as Eq. (23), Where i_1~i_4 are given values 0 or 1. Here, 0 means the auxiliary process is closing while 1 means opening.

$$P_{\text{auxiliary}} = P_{\text{cool}} \times i_1 + P_{\text{chip\_remove}} \times i_2 + P_{\text{tool}} \times i_3 + P_{\text{light}} \times i_4 \tag{23}$$

2.2 Improved cutting power model and some considerations

In order to forecast machine tool energy consumption more accurately in the cutting process, this paper puts forward an improved cutting power model of the milling machine. Some considerations are given as follows:

(1) Models proposed by Li et al. [23] and Gutowski et al. [20] as Eqs. (9)–(12) are easy to understand and easy to convert to SEC which can be used to estimate cutting energy consumption conveniently. Though some studies have pointed out that the same MRR obtained by different cutting parameters usually cause different cutting power. However, there are still lack discussion and experimental research about the relationship among cutting parameters, MRR, SEC, P_{cut}, and P_{material} in detail. This makes the models like Eqs. (9)–(12) remain to be illustrated in the accuracy of the energy consumption prediction of cutting process.

(2) The MRR for turning progress is calculated using Eq. (21), v_c is cutting speed, which is the rotational linear velocity of the workpiece. v_c implies a relationship between the rotation speed n and workpiece diameter (D), so P_{material} considers n in terms of the turning process. However, the MRR for a plane milling process is calculated using Eq. (22). v_f is the movement speed of milling cutter relative to the workpiece. In this instance, when cutting tool diameter d is given, the cutting speed v_c depends on the speed of n in the milling process. While Li et al.'s [23] milling power model, as Eq. (12), does not consider the effects of rotation speed n on P_{material}. Hence, this paper assumes that P_{material} is a function associated with n, namely $P_{\text{material}} = f(n, \text{MRR})$ or $P_{\text{material}} = f(n, a_p, a_e, v_f)$.

(3) Because the feed power is very small during the milling process, it can be neglected in the cutting power calculation. Namely, the cutting power of milling process is

$$P_{\text{cut}} = P_{\text{standby}} + P_{\text{spindle}}(n) + P_{\text{material}} \tag{24}$$

The SEC model of the milling process can be derived as

$$\text{SEC} = \frac{P_{\text{cut}}}{\text{MRR}} = \frac{P_{\text{standby}} + P_{\text{spindle}}(n) + P_{\text{material}}}{\text{MRR}} \tag{25}$$

(4) In order to validate the accuracy of the improved cutting power model, this paper will study the results of three groups of experiments. The first group consists of 35 tests through our work, the second group consists of 9 tests through our work, and the third group consists of 18 tests whose data is collected from Table 2 of Li et al. [23]. The improved model and models of Gutowsk et al. [20] and Li et al. [23] are compared by examining the results of the three groups of data individually to determine if increased accuracy was achieved.

(5) The cutting power test experiments were conducted using a cemented carbide vertical milling cutter to conduct plane milling on no. 45 steel. In consideration, the carbide material is widely used in production of all kinds of cutting tools. Carbide material expands the machineable material ranges of the same cutting tool; no. 45 is a kind of common carbon structural steel, which is widely used in mechanical processing and has a good cutting performance.

3 Experimental details

The experiments collected energy consumption data (power, current, voltage information, etc.) of a CNC milling machine (XKA714B/B) by using a Yokogawa CW240 clamp-type power meter. These energy consumption data were read and analyzed by using accessory analysis software APE240. Related machine tool and experimental platform are illustrated in Fig. 1, and experimental equipment details are given in Table 1.

3.1 Standby power and auxiliary power

When the machine tool starts, test its standby power and auxiliary power under the condition of stable, collect the energy consumption data in 1 min, respectively, then calculate the mean as $P_{standby}$ = 0.63 kW, P_{cool} = 0.26 kW, P_{tool} = 0.66 kW, and P_{light} = 0.05 kW. This machine tool has no automatic tool change function and chip removal function. P_{tool} is power of the cutter's hydraulic clamping device in loosened state.

3.2 Idle power

The machine tool is tested when spindle speed accelerates from 0 r/min to a constant rotation speed n (r/min); the energy consumption data are collected in 1 min, respectively. The average value of test results can be seen in Tables 2 and 3.

The parameters of the spindle power model are determined by fitting the data in Table 2 according to Eq. (17). The fitting results are shown in Fig. 2, namely:

$$P_{\text{spindle}}(n) = 0.0497 + 2.19479 \times 10^{-4} \times n$$

Generally, if the absolute value of correlation coefficient R-square is in range of 0.9 to 1, it can be concluded linear correlation is strong between regression variables. The correlation coefficient R-square is 0.99196, demonstrating a strong linear correlation and the effectiveness of the established spindle power formula under no load.

Next, the feed speed it set some value from 100 to 1000 (mm/min) to test the feed power of the x/y/z-axes. Table 3 shows the results of the slow feed power experimental data. With the x/y-axes feed speed increasing gradually, change of the feed power is not very obvious. The feed power of the z-axis in the upward direction is larger than that of the other direction, because more energy is needed to overcome friction and gravity. However the feed power accounted for a very small proportion of the total input power of this machine tool. Hence, it can be

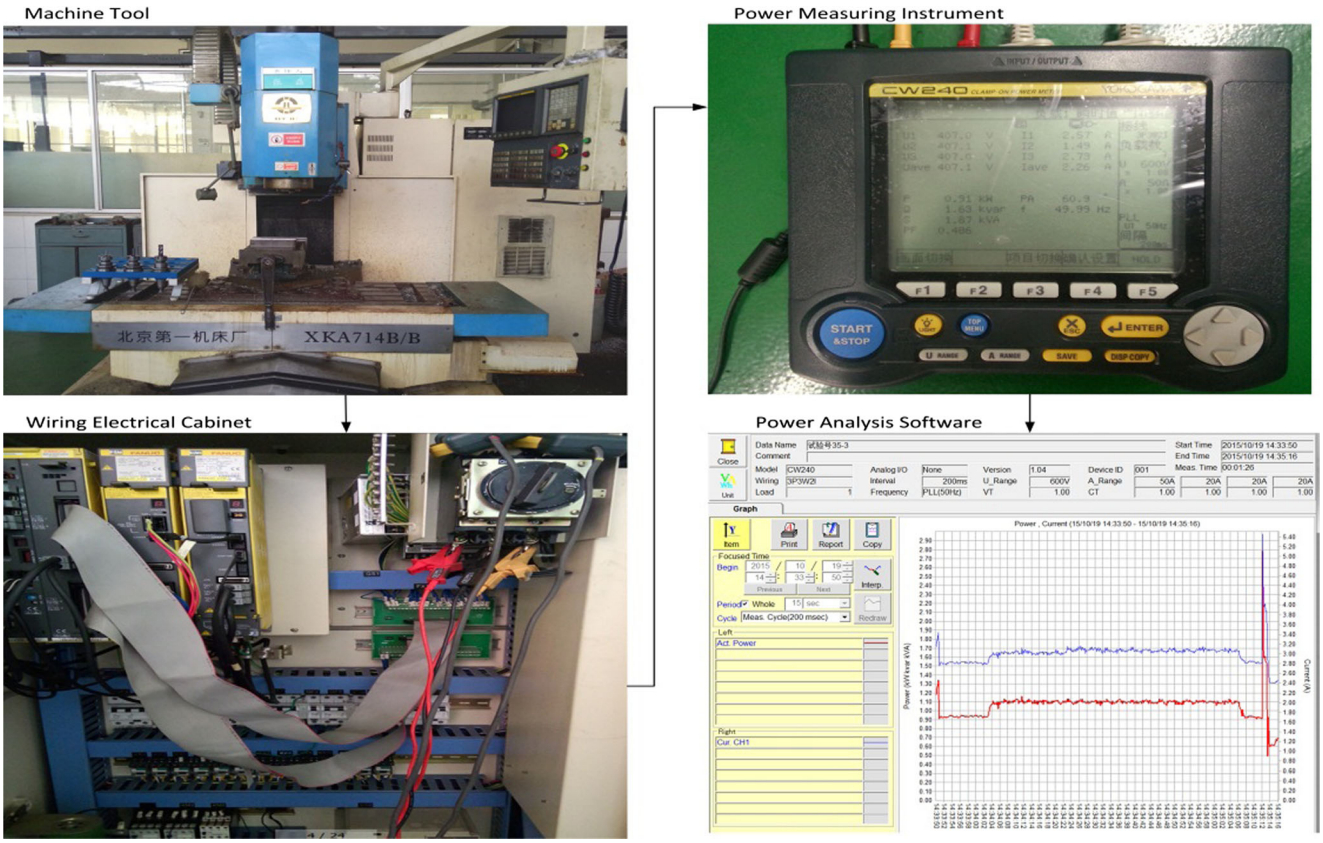

Fig. 1 Machine tool to be tested and experimental platform

Table 1 The experimental equipment details

Name	Information	
Cutting tool	Brand	GM-4E-D12.0 (Zhuzhou Cemented Carbide Cutting Tools Co., Ltd)
	Cutter diameter	12 mm
	Cutter coating	TiAlN
	Number of teeth	4
	Spiral angle	45°
	Cutter material	Carbide material
	Proper material to cut	Carbon steel, alloy steel, and cast iron
Cutting material	Grade	45
	Chemical composition mass fraction	
	C	0.42~0.50%
	Si	0.17~0.37%
	Mn	0.50~0.80%
	Cr	≤0.25%
	Ni	≤0.30%
	Cu	≤0.25%
	The mechanical properties of	σ_b/MPa = 600
	The mechanical properties of	σ_s/MPa = 355
	Delivery status without heat treatment, steel hardness of HBS ≤229	
Machine tool	Brand	XKA714B/B (Beijing no. 1 Machine Tool Plant)
	Table area (width × length)	400 × 1100 mm
	x-axis stroke	600 mm
	y-axis stroke	450 mm
	z-axis stroke	500 mm
	Spindle speed	100~5000 mm/min
	Feed rate	6~3200 mm/min (X/Y); 3~1600 mm/min (Z)
	Fast moving speed	8000 mm/min (X/Y); 4000 mm/min (Z)
	Positioning accuracy	±0.015 mm
	Spindle motor rated power	5.5/7.5 kW
	Spindle torque	220 Nm
	Feed torque	14 Nm
	Weight	3800 kg
	Outline dimension	2130 × 1700 × 2380 mm
Power instrument	YOKOGAWA CW240	
Power analysis software	APE240	
Sample frequency	100 ms	
Data fitting analysis tool	Origin8	

Table 2 Spindle power experimental results under no load

n (r/min)	500	700	1100	1500	1900	2300	2700	3100	3500	3900
P_{idle} (kw)	0.81	0.86	0.92	0.97	1.09	1.17	1.26	1.35	1.45	1.57
$P_{spindle}$ (kw)	0.18	0.23	0.29	0.34	0.46	0.54	0.63	0.72	0.82	0.94
Acceleration time (ms)	400	1400	2700	3700	4700	5800	6600	7600	8600	9500
Max P_{idle} (kw)	1.14	1.17	1.23	1.45	1.65	1.88	2.07	2.28	2.49	2.78
Max $P_{spindle}$ (kw)	0.51	0.54	0.60	0.82	1.02	1.25	1.44	1.65	1.86	2.15

Table 3 Feed power experimental results under no load

v_f (mm/min)	100	200	300	400	500	600	700	800	900	1000
P_{feed} (kw)										
x-axis	0.006	0.006	0.007	0.007	0.007	0.008	0.008	0.009	0.011	0.01
y-axis	0.008	0.009	0.01	0.015	0.018	0.021	0.021	0.025	0.027	0.029
z-axis (up)	0.067	0.071	0.079	0.085	0.088	0.091	0.093	0.097	0.13	0.14
z-axis (down)	0.018	0.019	0.021	0.021	0.021	0.022	0.022	0.021	0.021	0.022

regarded as constant C. According to the experimental results, the average values of feed shaft power in each direction as: $P_{feed-Y}=0.018$ kW, $P_{feed-X}=0.0079$ kW, $P_{feed-Zdown}=0.0208$ kW, and $P_{feed-Zup}=0.094$ kW.

3.3 Cutting power

To explore the relationships among the spindle rotation speed n, cutting parameters, the MRR, SEC, P_{cut}, and $P_{material}$, the experiment is designed utilizing Table 4. The relationship between n and power can be obtained by comparing horizontal items in Table 4. In the middle of Table 4, the same MRR is obtained by changing cutting parameters in column items, which are used to compare the changes in a machine tool's power. Table 5 shows the experimental results of Table 4 for the first set of 35 tests.

An orthogonal experiment with four factors and three levels is designed in Table 6 for the range analysis of cutting parameters on P_{cut} and $P_{material}$. Table 7 shows the experimental results of Table 6 (the second group consists of nine tests). Where $k1$~$k3$ are arithmetic mean of the results of P_{cut} test in any columns in Table 7 while the factor at the case of level ith, and the $R1$ is the range of factor about the P_{cut}, respectively. Where $k1'$~$k3'$ are arithmetic mean of the results of $P_{material}$ test in any columns in Table 7 while the factor at the case of level ith, and the $R2$ is the range of factor about the $P_{material}$, respectively. $P_{material}$ is calculated indirectly with the difference between P_{cut} the P_{idle}. Figure 3 shows the milling process and cutting tool path.

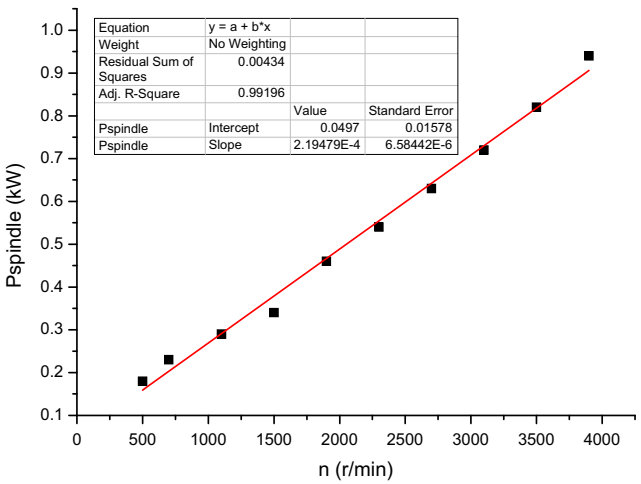

Fig. 2 Spindle power fitting curve under no load

The experimental data of the first group (fir-g), second group (sec-g), and third group (thi-g; the third group is consist of 18 tests referring to Table 2 from Li et al. [23]) are analyzed using the existing model based on Gutowski et al. [20] and Li et al. [23], and the proposed model of SEC and P_{cut}, respectively, and in order to analyze and compare the results of fitting, a flow chart in Fig. 4 shows how these models are being compared. For convenience, these models are renamed respectively as follows:

A. Model of Gutowski et al. [20]: $P_{cut}1=P_{idle}+c_1\times \mathrm{MRR}$ and $\mathrm{SEC1}=c_1'+\frac{c_2'}{\mathrm{MRR}}$
B. Model of Li et al. [23]: $P_{cut}2=c_1+c_2\times n+c_3\times \mathrm{MRR}$ and $\mathrm{SEC2}=c_1'+\frac{c_2'\times n}{\mathrm{MRR}}+\frac{c_3'}{\mathrm{MRR}}$
C. Proposed model (considering the effect of n on $P_{material}$):

$$P_{cut}3=c_1+c_2\times n+c_3\times n^{c_4}\times \mathrm{MRR} \text{ and } \mathrm{SEC3}=c_1'\times n^{c_2'}+\frac{c_3'\times n}{\mathrm{MRR}}+\frac{c_4'}{\mathrm{MRR}}$$

$$P_{cut}4=c_1+c_2\times n+c_3\times n^{c_4}\times {v_f}^{c_5}\times {a_p}^{c_6}\times {a_e}^{c_7} \text{ and } \mathrm{SEC4}=\frac{c_1'}{\mathrm{MRR}}+\frac{c_2'\times n}{\mathrm{MRR}}+\frac{c_3'\times n^{c_4'}\times {v_f}^{c_5'}\times {a_p}^{c_6'}\times {a_e}^{c_7'}}{\mathrm{MRR}}$$

Table 4 Factor and level design in experiment (the first group)

	n = 500 (r/min)	n = 900	n = 1300	n = 1700	n = 2100	v_f (mm/min)	a_p (mm)	a_e (mm)
MRR (mm^3/s)	18	18	18	18	18	120	1.5	6
	42	42	42	42	42	140	2	9
	4	4	4	4	4	160	0.5	3
	18	18	18	18	18	180	2	3
	10	10	10	10	10	200	1	3
	33	33	33	33	33	220	1.5	6
	18	18	18	18	18	240	0.5	9

Table 5 The experimental results of the first group

Test no.	n	v_f	a_p	a_e	MRR (mm^3/s)	$P_{spindle}$ (kW)	P_{idle} (kW)	P_{cut} (kW)	$P_{material}$ (kW)	SEC (J/mm^3)
1	500	140	2	9	42	0.18	0.81	0.93	0.12	22.143
2	900	140	2	9	42	0.26	0.89	1	0.11	23.810
3	1300	140	2	9	42	0.31	0.94	1.1	0.16	26.190
4	1700	140	2	9	42	0.42	1.05	1.19	0.14	28.333
5	2100	140	2	9	42	0.50	1.13	1.29	0.16	30.714
6	500	180	2	3	18	0.18	0.81	0.89	0.08	49.444
7	900	180	2	3	18	0.26	0.89	0.92	0.03	51.111
8	1300	180	2	3	18	0.31	0.94	1.03	0.09	57.222
9	1700	180	2	3	18	0.42	1.05	1.13	0.08	62.778
10	2100	180	2	3	18	0.50	1.13	1.22	0.09	67.778
11	500	120	1.5	6	18	0.18	0.81	0.89	0.08	49.444
12	900	120	1.5	6	18	0.26	0.89	0.93	0.04	51.667
13	1300	120	1.5	6	18	0.31	0.94	1.03	0.09	57.222
14	1700	120	1.5	6	18	0.42	1.05	1.13	0.08	62.778
15	2100	120	1.5	6	18	0.50	1.13	1.24	0.11	68.889
16	500	220	1.5	6	33	0.18	0.81	0.91	0.1	27.576
17	900	220	1.5	6	33	0.26	0.89	0.98	0.09	29.697
18	1300	220	1.5	6	33	0.31	0.94	1.09	0.15	33.030
19	1700	220	1.5	6	33	0.42	1.05	1.19	0.14	36.061
20	2100	220	1.5	6	33	0.50	1.13	1.3	0.17	39.394
21	500	200	1	3	10	0.18	0.81	0.89	0.08	89.000
22	900	200	1	3	10	0.26	0.89	0.93	0.04	93.000
23	1300	200	1	3	10	0.31	0.94	0.99	0.05	99.000
24	1700	200	1	3	10	0.42	1.05	1.09	0.04	109.000
25	2100	200	1	3	10	0.50	1.13	1.19	0.06	119.000
26	500	160	0.5	3	4	0.18	0.81	0.87	0.06	217.500
27	900	160	0.5	3	4	0.26	0.89	0.92	0.03	230.000
28	1300	160	0.5	3	4	0.31	0.94	0.98	0.04	245.000
29	1700	160	0.5	3	4	0.42	1.05	1.06	0.01	265.000
30	2100	160	0.5	3	4	0.50	1.13	1.15	0.02	287.5
31	500	240	0.5	9	18	0.18	0.81	0.89	0.08	49.444
32	900	240	0.5	9	18	0.26	0.89	0.93	0.04	51.667
33	1300	240	0.5	9	18	0.31	0.94	1.01	0.07	56.111
34	1700	240	0.5	9	18	0.42	1.05	1.12	0.07	62.222
35	2100	240	0.5	9	18	0.50	1.13	1.21	0.08	67.222

The fitting coefficient results are shown in Tables 8 and 9. ANOVA results of these models are shown in Tables 10 and 11. Where c_1~c_7 and c'_1~c'_7 are fitting coefficients, R-sq. is correlation coefficient R-square (Adj), SS is sum of square, MS is mean square, F is F value, and P is prob > F.

3.4 Cutting power model validation and comparison

The experimental conditions of the first group are consistent with the second group in this paper. Fitting coefficient results of P_{cut} and SEC of the first group are used to predict tests no. 3 and no. 4 of the second group. The predicted values and the accuracy of different fitting models are shown in Table 12 and Fig. 5.

Table 6 Factors and levels design in orthogonal experimental (the second group)

Factor v_f (mm/min)	Level	Factor a_p (mm)	Level	Factor a_e (mm)	Level	Factor n (r/min)	Level
v_{f1}	120	a_{p1}	0.5	a_{e1}	3	n_1	500
v_{f2}	180	a_{p2}	1.5	a_{e2}	6	n_2	1300
v_{f3}	240	a_{p3}	2	a_{e3}	9	n_3	2100

Table 7 The experimental results of the second group

Test no.	v_f	a_p	a_e	n	MRR (mm^3/s)	P_{idle} (kW)	P_{cut} (kW)	$P_{material}$ (kW)	SEC (J/mm^3)
1	120	0.5	3	500	3	0.81	0.83	0.02	276.667
2	120	1.5	6	1300	18	0.94	1.03	0.09	57.222
3	120	2	9	2100	36	1.13	1.36	0.23	37.778
4	180	0.5	6	2100	9	1.13	1.17	0.04	130.000
5	180	1.5	9	500	40.5	0.81	0.95	0.14	23.457
6	180	2	3	1300	18	0.94	1.03	0.09	57.222
7	240	0.5	9	1300	18	0.94	1.01	0.07	56.111
8	240	1.5	3	2100	18	1.13	1.24	0.11	68.889
9	240	2	6	500	48	0.81	0.96	0.15	20.000
$k1$	1.073	1.003	1.033	0.913					
$k2$	1.05	1.073	1.053	1.023					
$k3$	1.07	1.117	1.107	1.257	Range about the P_{cut}: $n > a_p > a_e > v_f$				
R1	0.023	0.114	0.074	0.344					
$k1'$	0.113	0.043	0.073	0.103					
$k2'$	0.09	0.113	0.093	0.083					
$k3'$	0.11	0.157	0.147	0.127	Range about the $P_{material}$: $a_p > a_e > n > v_f$				
R^2	0.023	0.114	0.074	0.044					

According to Table 12, it can be seen that the proposed model SEC3 and $P_{cut}3$ have a higher predicting accuracy compared with other models. From Tables 8, 9, 10, and 11, it can also be found that the optimal fitting correlation models are SEC3 and $P_{cut}3$, due to considering n's effect on $P_{material}$ in the milling process.

(1) In the first group experiments:

R-sq. Adj(SEC3) = 0.9996 > R-sq. Adj(SEC2) = 0.9993 > R-sq. Adj(SEC1) = 0.97424

R-sq. Adj($P_{cut}3$) = 0. 97653 > R-sq.Adj($P_{cut}2$) = 0.97088 > R-sq.Adj($P_{cut}1$) = 0.96228

(2) In the second group experiments:

R-sq. Adj(SEC3) = 0.99975 > R-sq. Adj(SEC2) = 0.9996 > R-sq. Adj(SEC1) = 0.97618

R-sq. Adj($P_{cut}3$) = 0.97724 > R-sq.Adj($P_{cut}2$) = 0.95819 > R-sq.Adj($P_{cut}1$) = 0.94636

(3) In the third group experiments:

R-sq. Adj(SEC3) = 0.99983 = R-sq. Adj(SEC2) = 0.99983 > R-sq. Adj(SEC1) = 0.97463

R-sq. Adj($P_{cut}3$) = 0.99983 > R-sq.Adj($P_{cut}2$) = 0.99355 > R-sq.Adj($P_{cut}1$) = 0.98395

However, for the proposed model $P_{cut}4$, R-sq.Adj($P_{cut}4$)0.98071 > R-sq.Adj($P_{cut}3$) = 0.97653 in the first group experiments and R-sq. Adj($P_{cut}4$) = 0.31083 < R-sq.Adj($P_{cut}3$) = 0.97724 in the

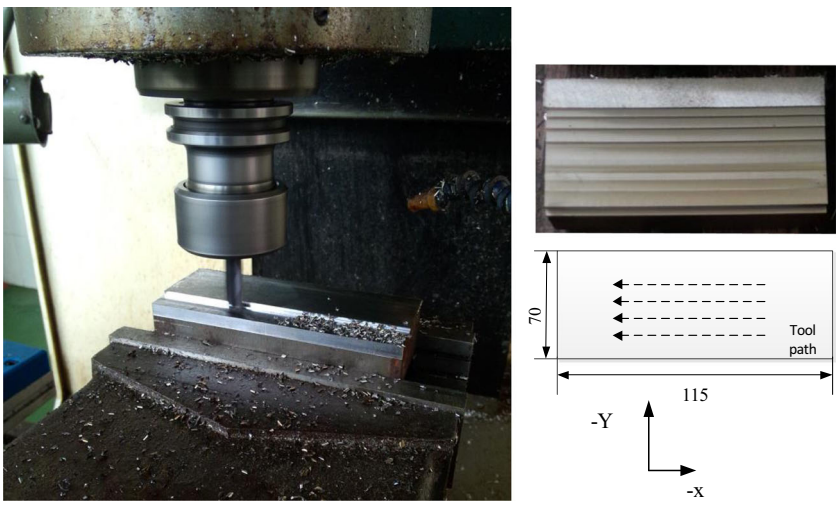

Fig. 3 Milling process and cutting tool path

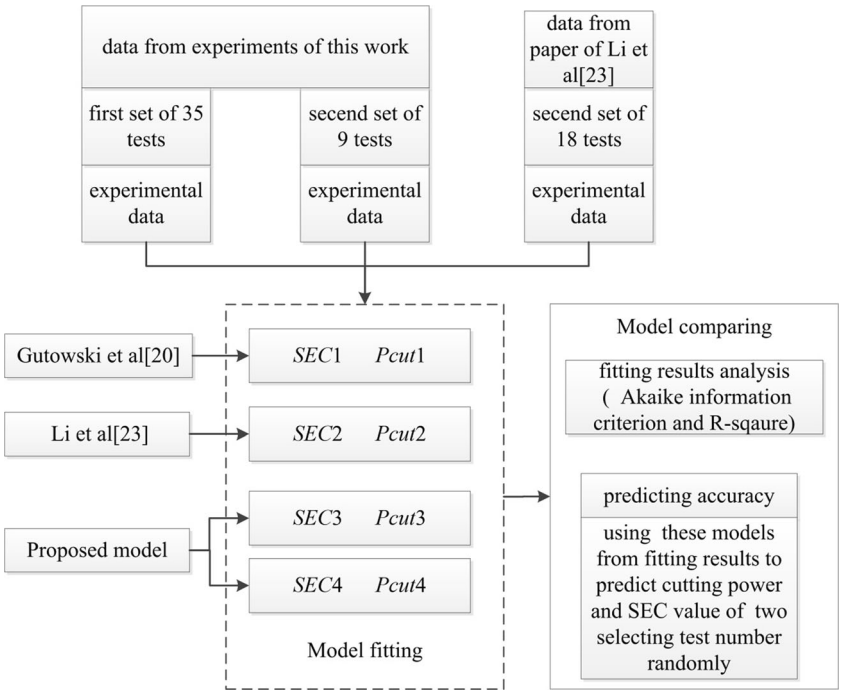

Fig. 4 Model comparing flow chart

second group experiments. This kind of phenomenon is because the model $P_{cut}4$ with independent variables of n, v_f, a_e, and a_p, needs to solve too many unknown coefficients. With only nine tests in the second group experiments, the fitting result of $P_{cut}4$ is not ideal. Whereas, it is appropriate to solve the seven unknown coefficients in the first group experiments through 35 tests data.

So, if using a small amount of experimental data to rapidly predict P_{cut} of a machine tool, the method using MRR as the independent variable shows a better data fit. Using MRR as the independent variable is recommended in instances with less experimental data because only a few unknown coefficients need to be solved. Also, $P_{material}$ takes up a small proportion of input power. Additionally, it is easy to get similar $P_{material}$ values for the same MRR while cutting parameters vary (in Table 13, variation of $P_{material}$ is small for the same MRR).

For SEC, differences in the fitting correlations between SEC3 and SEC4 are not obvious. This is because SEC mainly depends on MRR and n, and shows little sensitivity when considering v_f, a_e, and a_p.

In addition, Akaike information criterion (AIC) can estimate the quality of statistical models for given test data, and

Table 8 Fitting coefficient results of SEC1~SEC4

Model	Test	c_1	c_2	c_3	c_4	c_5	c_6	c_7	R-sq.
SEC1	fir-g	3.07462	984.03563	–	–	–		–	0.97424
SEC1	sec-g	14.19496	810.29243	–	–	–	–	–	0.97618
SEC1	thi-g	11.39887	614.02334	–	–	–	–	–	0.97463
SEC2	fir-g	3.07462	0.18259	746.66333	–	–	–	–	0.99933
SEC2	sec-g	3.40163	0.20435	716.65762	–	–		–	0.9996
SEC2	thi-g	5.1295	0.12986	478.52939	–	–	–	–	0.99983
SEC3	fir-g	5.72485×10^{-9}	785.64082	2.72708	0.1553		–	–	0.9996
SEC3	sec-g	0.54574	0.97826	0.17519	0.00385		–	–	0.99975
SEC3	thi-g	−0.02816	0.1121	0.12757	2.25423		–	–	0.99983
SEC4	fir-g	767.74494	0.18259	0.00657	−9.44931	−2.16739	−16.9579	13.12638	0.99826
SEC4	sec-g	1186.67551	0.83379	−20.51266	0.62167	−0.04324	−0.07143	−0.06917	0.99997
SEC4	thi-g	479.18895	0.12108	0.07085	0.24665	0.79883	0.81507	0.7688	0.9998

Table 9 Fitting coefficient results of $P_{cut}1 \sim P_{cut}4$

Model	Test	c'_1	c'_2	c'_3	c'_4	c'_5	c'_6	c'_7	*R*-sq.
$P_{cut}1$	fir-g	0.00374	–	–	–	–	–	–	0.96228
$P_{cut}1$	sec-g	0.00423	–	–	–	–	–	–	0.94636
$P_{cut}1$	thi-g	5.30536	–	–	–	–	–	–	0.98395
$P_{cut}2$	fir-g	0.70981	2.12857×10^{-4}	0.00293	–	–	–	–	0.97088
$P_{cut}2$	sec-g	0.65398	2.39865×10^{-4}	0.00426	–	–	–	–	0.95819
$P_{cut}2$	thi-g	478.45624	0.13194	4.86031	–	–	–	–	0.99355
$P_{cut}3$	fir-g	0.77593	1.65069×10^{-4}	7.57733×10^{-7}	1.13996	–	–	–	0.97635
$P_{cut}3$	sec-g	0.70944	1.82688×10^{-4}	1.11114×10^{-4}	0.54574	–	–	–	0.97724
$P_{cut}3$	thi-g	476.92624	0.13287	5.9889	−0.02816	–	–	–	0.99983
$P_{cut}4$	fir-g	0.87763	-5.09861×10^{-4}	1.45568×10^{-4}	1.16013	0.04321	0.05557	0.05176	0.98071
$P_{cut}4$	sec-g	0.78549	2.14583×10^{-4}	−0.00124	−11.95154	−3.01627	−10.2719	−8.58015	0.31083
$P_{cut}4$	thi-g	407.28526	0.11599	0.17144	0.27149	0.66506	0.62928	0.61987	0.99351

it can explain the tradeoff between the goodness of fit of models. The assumption is that the error of the model is independent of the normal distribution. Where *m* is number of the observation, the RSS is the sum of squares for error, and *k* is number of parameters, then:

$$\mathrm{AIC} = 2k + m2\ln\left(\mathrm{RSS}\Big/\mathrm{m}\right)$$

The preferred model should be the one with the smallest numerical AIC value. In this paper, AIC are used to compare different models using test data of the fir-g and sec-g. The calculated value of AIC can be seen in Table 13.

From Table 13, it can be seen that the SEC3 and $P_{cut}3$ models are intended to be better models in some degree,

Table 10 ANOVA results of SEC1~SEC4

Model	Test		*df*	SS	MS	*F* value	*P* value
SEC1	fir-g	Regression model	2	420,638.73061	210,319.3653	1523.28627	0.0000
		Residual	33	4556.29331	138.06949	–	–
SEC1	sec-g	Regression model	2	109,192.04059	54,596.02029	356.22153	0.0000
		Residual	7	1072.84964	153.26423	–	–
SEC1	thi-g	Regression model	2	154,466.73386	77,233.36693	1373.82985	0.0000
		Residual	16	899.48102	56.21756	–	–
SEC2	fir-g	Regression model	3	425,079.40091	141,693.13364	39,215.20999	0.0000
		Residual	32	115.623	3.61322	–	–
SEC2	sec-g	Regression model	3	110,249.58267	36,749.86089	14,404.58857	0.0000
		Residual	6	15.30756	2.55126	–	–
SEC2	thi-g	Regression model	3	155,360.72721	51,786.90907	141,554.38701	0.0000
		Residual	15	5.48767	0.36584	–	–
SEC3	fir-g	Regression model	4	425,128.58665	106,282.14666	49,591.84577	0.0000
		Residual	31	66.43726	2.14314	–	–
SEC3	sec-g	Regression model	4	110,256.94205	27,564.23551	17,339.97187	0.0000
		Residual	5	7.94818	1.58964	–	–
SEC3	thi-g	Regression model	4	155,360.84385	38,840.21096	101,240.06041	0.0000
		Residual	14	5.37103	0.38364	–	–
SEC4	fir-g	Regression model	7	424,933.52018	60,704.7886	6499.84622	0.0000
		Residual	28	261.50374	9.33942	–	–
SEC4	sec-g	Regression model	7	110,264.55868	15,752.07981	95,020.16825	0.0000
		Residual	2	0.33155	0.16578	–	–
SEC4	thi-g	Regression model	7	155,361.23409	22,194.46201	49,016.20371	0.0000
		Residual	11	4.98078	0.4528	–	–

Table 11 ANOVA results of $P_{cut}1$~$P_{cut}4$

Model	Test		*df*	SS	MS	*F* value	*P* value
$P_{cut}1$	fir-g	Regression model	1	38.86022	38.86022	61,811.26887	1
		Residual	34	0.02138	6.28692×10^{-4}	–	–
$P_{cut}1$	sec-g	Regression model	1	10.39954	10.39954	7259.86453	1
		Residual	8	0.01146	0.00143	–	–
$P_{cut}1$	thi-g	Regression model	1	1.01816×10^{7}	1.01816×10^{7}	111,008.01902	1
		Residual	17	1559.23805	91.71989	–	–
$P_{cut}2$	fir-g	Regression model	3	38.86607	12.95536	26,694.4458	0.0000
		Residual	32	0.01553	4.8532×10^{-4}	–	–
$P_{cut}2$	sec-g	Regression model	3	10.4043	3.4681	3106.5004	0.0000
		Residual	6	0.0067	0.00112	–	–
$P_{cut}2$	thi-g	Regression model	3	1.01826×10^{7}	3.39422×10^{6}	92,035.31661	0.0000
		Residual	15	553.19247	36.8795	–	–
$P_{cut}3$	fir-g	Regression model	4	38.86938	9.71734	24,650.02626	0.0000
		Residual	31	0.01222	3.94212×10^{-4}	–	–
$P_{cut}3$	sec-g	Regression model	4	10.40796	2.60199	4281.71105	0.0000
		Residual	5	0.00304	6.07699×10^{-4}	–	–
$P_{cut}3$	thi-g	Regression model	4	1.01826×10^{7}	2.54566×10^{6}	64,548.51215	0.0000
		Residual	14	552.13162	39.43797	–	–
$P_{cut}4$	fir-g	Regression model	7	38.8726	5.55323	17,273.36601	0.0000
		Residual	28	0.009	3.21491×10^{-4}	–	–
$P_{cut}4$	sec-g	Regression model	7	10.37419	1.48203	80.53283	0.01232
		Residual	2	0.03681	0.0184	–	–
$P_{cut}4$	thi-g	Regression model	7	1.01828×10^{7}	1.45468×10^{6}	39,198.03348	0.0000
		Residual	11	408.22285	37.11117	–	–

Table 12 Predicted values and the accuracy of different fitting models

Test no.	Measured value		Model	Predicted value	Accuracy	Model	Predicted value	Accuracy
sec-g.3	P_{cut} = 1.36	SEC = 37.778	$P_{cut}1$	1.2646	0.9299	SEC1	30.4089	0.8049
sec-g.3			$P_{cut}2$	1.2623	0.9282	SEC2	34.4664	0.9123
sec-g.3			$P_{cut}3$	1.2897	0.9483	SEC3	37.4549	0.9914
sec-g.3			$P_{cut}4$	1.1239	0.8264	SEC4	31.9773	0.8465
sec-g.4	P_{cut} = 1.17	SEC = 130	$P_{cut}1$	1.1637	0.9946	SEC1	112.4119	0.8647
sec-g.4			$P_{cut}2$	1.1832	0.9887	SEC2	128.6415	0.9896
sec-g.4			$P_{cut}3$	1.1644	0.9952	SEC3	130.1025	0.9992
sec-g.4			$P_{cut}4$	1.1818	0.9899	SEC4	127.9093	0.9839

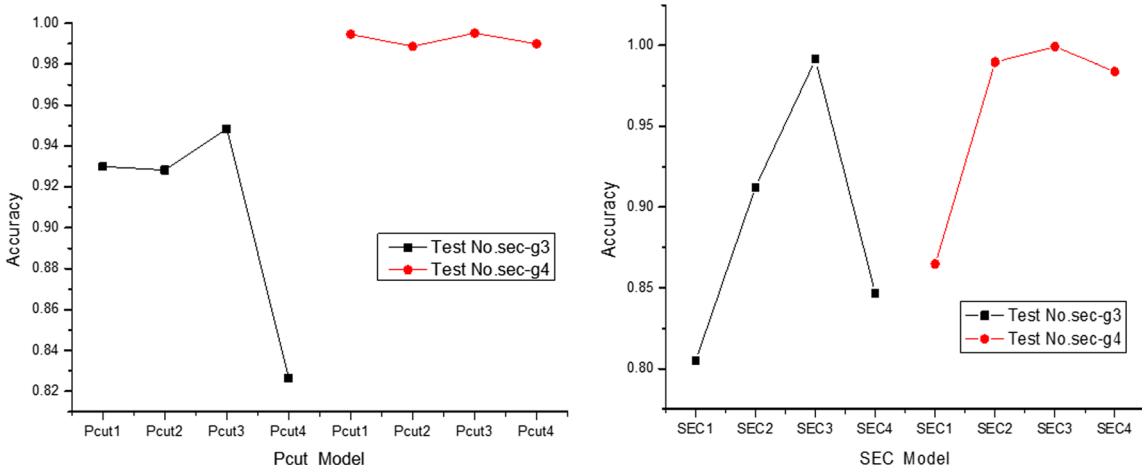

Fig. 5 Accuracy compared of each model

because of their lower AIC value. For the $P_{cut}4$ model, a large number of experimental observations gives a better data fit, but fewer observations gives an unsatisfactory result. Moreover, SEC4 is unstable when the number of the observation changed. The results found in Table 13 are consistent with the conclusions of the *R*-square analysis.

4 Analysis and discussion

According to Table 2, when spindle speed accelerates from 0 r/min to a constant rotation speed n (r/min), it forms a linear relationship with the maximum $P_{spindle}$ in acceleration process, $P_{spindle}$, acceleration time t_a have a linear relationship with spindle rotation speed n in general, as found in Fig. 6.

From Table 5, it can be found that a linear relationship exists between P_{cut} and n, as shown in Fig. 7. Because of the variable power of the machine tool, $P_{spindle}$ demonstrates linear growth along with n and $P_{material}$ accounts only a small portion of the total input power. In experiments of the first group, $P_{material}$ is 7.84% of P_{cut}, on average. In addition, the SEC also increases with increasing n.

Following Table 5, it can also be found that $P_{material}$ is significantly affected by the n, as shown in Fig. 8. The points and line of the same color in Fig. 8 imply the same cutting parameters v_f, a_p and a_e (namely the same MRR) but different n. When n changes, $P_{material}$ changes as well, but this change is not a linear relationship. For points and line of the same color in Fig. 8, when n increased from 500 to 2100 r/min, $\Delta P_{material}(\max P_{material} - \min P_{material})$ has a floating range of 0.04~0.08 kW. For example, at the line of v_f = 240 mm/min, v_f = 0.04 kW; while at the line

Table 13 AIC value of different model

AIC value	Model	Group	k	m	RSS
172.41208	SEC1	fir-g	1	35	4556.29331
45.82454	SEC2	fir-g	2	35	115.62300
26.43185	SEC3	fir-g	2	35	66.43726
80.38852	SEC4	fir-g	5	35	261.50374
45.02764	SEC1	sec-g	1	9	1072.84964
8.78010	SEC2	sec-g	2	9	15.30756
2.88147	SEC3	sec-g	2	9	7.94818
−19.71081	SEC4	sec-g	5	9	0.33155
−122.43718	$P_{cut}1$	fir-g	1	35	1.00000
−266.21154	$P_{cut}2$	fir-g	2	35	0.01553
−274.60103	$P_{cut}3$	fir-g	2	35	0.01222
−281.30576	$P_{cut}4$	fir-g	4	35	0.00900
−57.99505	$P_{cut}1$	sec-g	1	9	0.01146
−60.82585	$P_{cut}2$	sec-g	2	9	0.00670
−67.93810	$P_{cut}3$	sec-g	2	9	0.00304
−41.49289	$P_{cut}4$	sec-g	4	9	0.03681

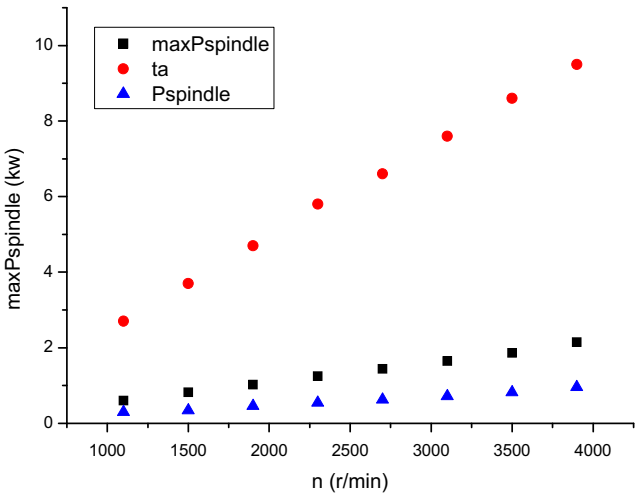

Fig. 6 Relation between n and max $P_{spindle}/P_{spindle}/t_a$

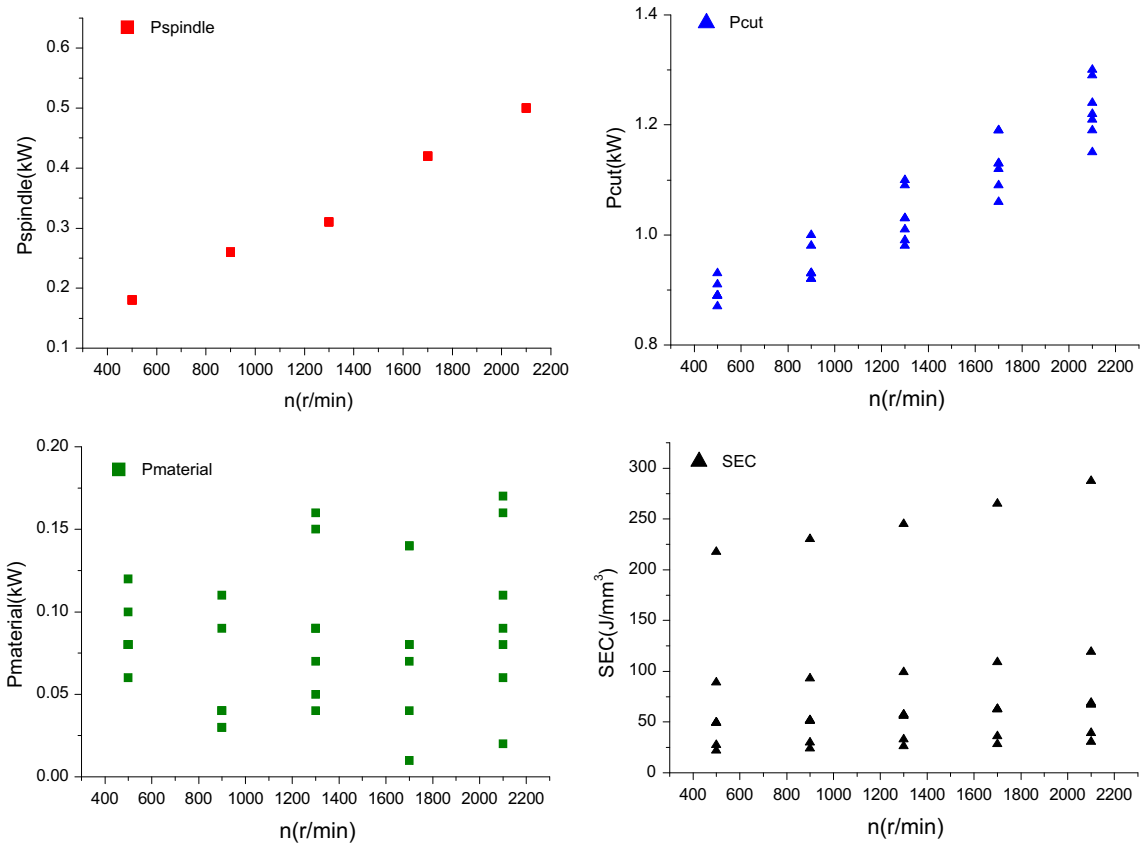

Fig. 7 Relation between n and $P_{cut}/P_{material}/P_{spindle}$/SEC

of v_f = 220 mm/min, $\Delta P_{material}$ = 0.08 kW. This float has obvious influence on $P_{material}$, and it should not be ignored. For some rotation speed n, $P_{material}$ presents a downward trend, which may be due to obtaining a more suitable cutting speed v_c under that particular n during the milling process.

Relationship between MRR and SEC from Table 5 is shown in Fig. 9. MRR is inversely proportional with SEC on the whole. However, the same MRR does not necessarily get the same SEC. For instance, when MRR = 4 mm^3/s, as n grows from 500 to 2100 r/min, ΔSEC(maxSEC − min SEC) = 287.5–217.5 = 70 J/mm^3,

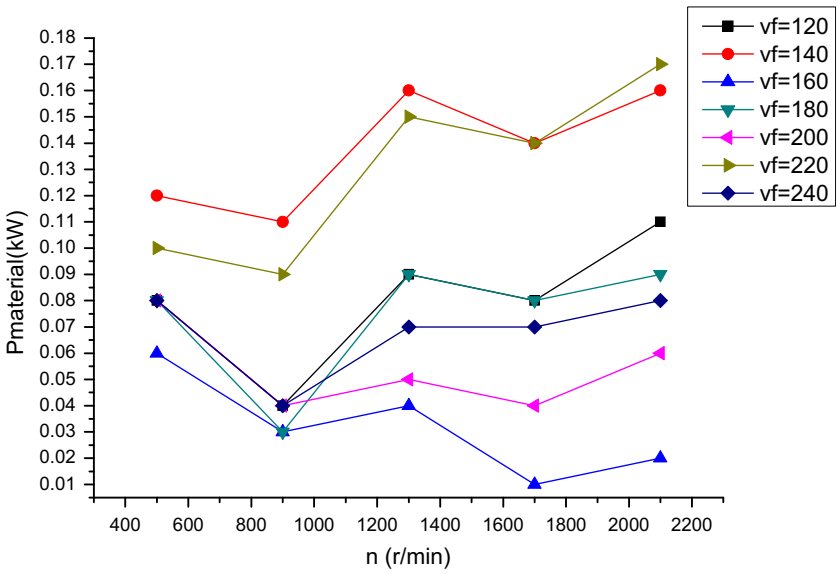

Fig. 8 Relation between n and $P_{material}$

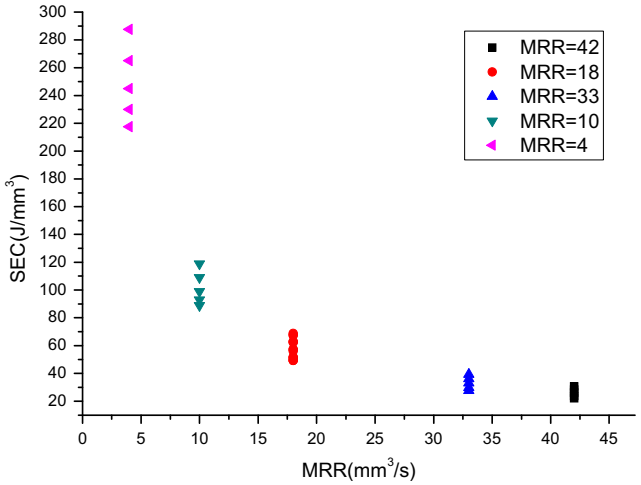

Fig. 9 Relation between MRR and SEC

namely the SEC's growth rate is 32.2%; when MRR = 10 mm^3/s, ΔSEC = 119–89 = 30 J/mm^3, the SEC's growth rate is 33.7%; similarly, when MRR = 18 mm^3/s, the SEC's growth rate is 39.3%; when MRR = 33 mm/s, the SEC's growth rate is 42.8%; and when MRR = 42 mm^3/s, the SEC's growth rate is 38.7%.

According to Table 5, relationships between MRR, $P_{material}$, and P_{cut} can be found in Fig. 10. With MRR increasing, P_{cut} and $P_{material}$ show the tendency of increase in general. Further, find out all experimental data of the first and second groups at the MRR = 18 mm^3/s as shown in Table 14. Taking the same cutting parameters v_f, a_e and a_p as the same level, W, in Table 14. Getting a similar level of $P_{material}$ when MRR is the same can be done by changing the W under the same n. $P_{material}$ is not completely the same, but the changes in $P_{material}$ are minute.

Table 14 Experiment results of fir-g and sec-g at MRR = 18 mm^3/s

Test no.	n (r/min)	W	MRR (mm^3/s)	P_{cut} (kW)	$P_{material}$ (kW)
fir-g.6	500	$W1$	18	0.89	0.08
fir-g.11	500	$W2$	18	0.89	0.08
fir-g.31	500	$W3$	18	0.89	0.08
fir-g.7	900	$W1$	18	0.92	0.03
fir-g.12	900	$W2$	18	0.93	0.04
fir-g.32	900	$W3$	18	0.93	0.04
fir-g.8	1300	$W1$	18	1.03	0.09
fir-g.13	1300	$W2$	18	1.03	0.09
fir-g.33	1300	$W3$	18	1.01	0.07
fir-g.9	1700	$W1$	18	1.13	0.08
fir-g.14	1700	$W2$	18	1.13	0.08
fir-g.34	1700	$W3$	18	1.12	0.07
fir-g.10	2100	$W1$	18	1.22	0.09
fir-g.15	2100	$W2$	18	1.24	0.11
fir-g.35	2100	$W3$	18	1.21	0.08
sec-g.8	2100	$W4$	18	1.24	0.11

Note:

$W1$: $v_f = 180$ mm/ min , $a_p = 2$ mm , $a_e = 3$ mm

$W2$: $v_f = 120$, $a_p = 1.5$, $a_e = 6$

$W3$: $v_f = 240$, $a_p = 0.5$, $a_e = 9$

$W4$: $v_f = 240$, $a_p = 1.5$, $a_e = 3$

The range of factors n, a_p, a_e, and v_f about P_{cut} and $P_{material}$ are shown in Table 7. The degree of influence of the various factors about P_{cut} can be ordered as follows: $n > a_p > a_e > v_f$. The degree of influence of the various factors about $P_{material}$ can be ordered as follows: $a_p > a_e > n > v_f$. A trend chart between the factors and indices can be found in Figs. 11 and 12. Of these, n has influence on $P_{material}$.

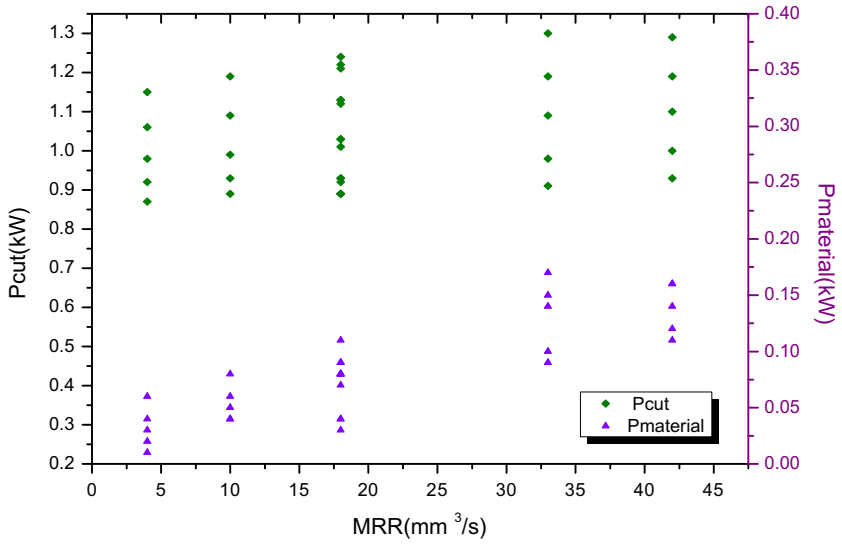

Fig. 10 Relation between MRR and $P_{cut}/P_{material}$

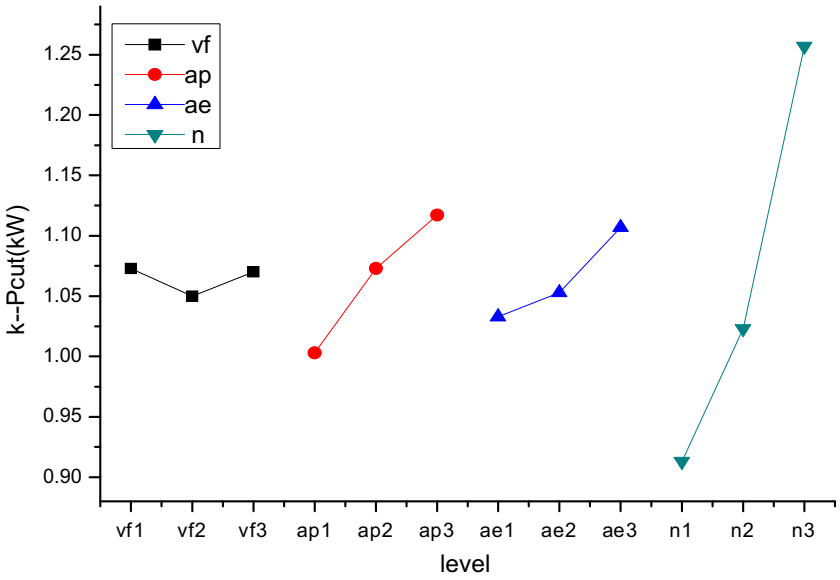

Fig. 11 Trend chart (relation between factors and indexes P_{cut})

5 Conclusion

Establishing a rapid, accurate, and practical energy consumption evaluation model for a machine tool is necessary for the manufacturing industry to save energy and increase profits. For this purpose, the SEC model of machine tools was developed and widely used. This paper discusses the relationships between n, cutting parameter (v_f, a_e, and a_p), MRR and SEC, P_{cut}, and $P_{material}$ using experimental methods. This was accomplished by substituting three groups of experimental data into different SEC and P_{cut} models and analyzing the fitting results. The main conclusions are as follows:

(1) In the process of milling, actual measured P_{cut} is different when using different combination of v_f, a_e, and a_p to get the same MRR. Changes in n cause changes in $P_{spindle}$ and $P_{material}$. On the other hand, when n is the same, different combinations of v_f, a_e, and a_p cause changes in $P_{material}$ values, but this change is minute.

(2) The model considering v_f, a_e, and a_p as independent variables can improve the accuracy of predicting P_{cut}, but this accuracy depends on a large amount of experimental data. The reason is that there are many unknown coefficients in the formulas, so less experimental data may lead to the unsatisfactory fitting and prediction of results. The model considering MRR as independent variable can get a better fitting result to predict P_{cut}, while using less data in an orthogonal experiment. Hence, using MRR is a rapid energy consumption evaluation method.

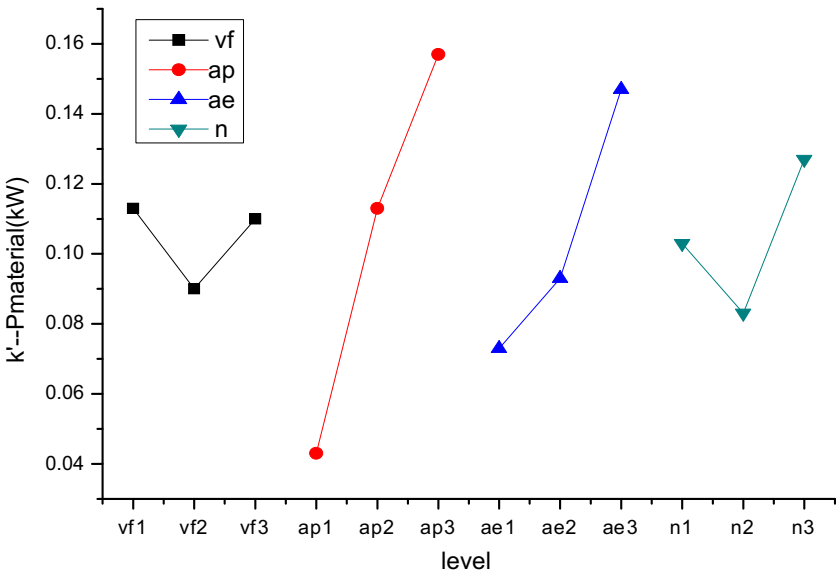

Fig. 12 Trend chart (relation between factors and indexes $P_{material}$)

Considering that $P_{material}$ and P_{cut} have small changes when using the same MRR by combining different of v_f, a_e, and a_p. In addition, SEC mainly depends on MRR and n and shows little sensitivity with regards to v_f, a_e, and a_p.

(3) The improved model SEC3 and $P_{cut}3$ demonstrate better fitting correlation when compared with other models using the different groups of experimental data. The proposed model put forward in this work which considers the influence of n on $P_{material}$, increases the accuracy of predicting cutting power in a milling process.

Acknowledgements This research is funded by the National High Technology Research and Development Program (no. 2014AA041503). Ziwu Liu is thanked for providing valuable insight and advice.

References

1. Peng T, Xu X (2014) Energy-efficient machining systems: a critical review. Int J Adv Manuf Technol 72(9–12):1389–1406. doi:10.1007/s00170-014-5756-0
2. US Energy Information Administration (EIA) Annual Energy outlook 2015 with projections to 2040, http://www.eia.gov/forecasts/aeo/. Accessed 25 April 2016
3. National Bureau of Statistics of the People's Republic of China http://data.stats.gov.cn/adv.htm?m=advquery&cn=C01. Accessed 25 April 2016
4. Cao HJ, Li HC, Du YB, Li XG (2012) Current situation and development trend of low-carbon manufacturing. Aeronaut Manuf Technol 9:26–31. doi:10.16080/j.issn1671-833x.2012.09.014 (in Chinese)
5. Zhou LR, Li JF, Li FY, Meng Q, Li J, Xu XS (2016) Energy consumption model and energy efficiency of machine tools: a comprehensive literature review. J Clean Prod 112(Part 5):3721–3734. doi:10.1016/j.jclepro.2015.05.093
6. Duflou JR, Sutherland JW, Dornfeld D, Herrmann C, Jeswiet J, Kara S, Hauschild M, Kellens K (2012) Towards energy and resource efficient manufacturing : a processes and systems approach. CIRP Ann Manuf Technol 61(2):587–609. doi:10.1016/j.cirp.2012.05.002
7. Ma J, Ge X, Chang SI, Lei S (2014) Assessment of cutting energy consumption and energy efficiency in machining of 4140 steel. Int J Adv Manuf Technol 74:1701–1708
8. Gutowski T, Dahmus J, Thiriez A (2006) Electrical energy requirements for manufacturing processes. In: 13th CIRP international conference on life cycle engineering, Leuven, Belgium, pp. 623–628
9. ISO14955-1:2014. http://www.iso.org/iso/catalogue_detail?csnumber=55294. Accessed 25 April 2016
10. Zhang YJ (2014) Energy efficiency techniques in machining process: a review. Int J Adv Manuf Technol 71(5–8):1123–1132. doi:10.1007/s00170-013-5551-3
11. Sebastian T (2012) Energy Efficiency in Manufacturing systems. Springer, Germany
12. Mori M, Fujishima M, Inamasu Y, Oda Y (2011) A study on energy efficiency improvement for machine tools. CIRP Ann Manuf Technol 60(1):145–148. doi:10.1016/j.cirp.2011.03.099
13. Liu F, Liu S (2012) Multiperiod energy model of electromechanical main driving system during the service process of machine tools. J Mech Eng 21:132–140 (in Chinese)
14. Lv JX, Tang RZ, Jia S (2014) Therblig-based energy supply modeling of computer numerical control machine tools. J Clean Prod 65:168–177. doi:10.1016/j.jclepro.2013.09.055
15. Zhong QQ, Tang RZ, Lv JX, Jia S, Jin MZ (2016) Evaluation on models of calculating energy consumption in metal cutting processes: a case of external turing process. Int J Adv Manuf Technol 82:2087–2099
16. Munoz AA, Sheng P (1995) An analytical approach for determining the environmental impact of machining processes. J Mater Process Technol 53(3–4):736–758. doi:10.1016/0924-0136(94)01764-r
17. Kishawy HA, Kannan S, Balazinski M (2004) An energy based analytical force model for orthogonal cutting of metal matrix composites. CIRP Ann Manuf Technol 53(1):91–94
18. Shao H, Wang HL, Zhao XM (2004) A cutting power model for tool wear monitoring in milling. Int J Mach Tools Manuf 44(14):1503–1509. doi:10.1016/j.ijmachtools.2004.05.003
19. Yoon HS, Lee JY, Kim MS, Ahn SH (2014) Empirical power-consumption model for material removal in three-axis milling. J Clean Prod 78:54–62. doi:10.1016/j.jclepro.2014.03.061
20. Gutowski T, Branham M, Dahmu J, Jones A, Thiriez A (2009) Thermodynamic analysis of resources used in manufacturing processes. Environ Sci Technol 43(5):1584–1590. doi:10.1021/es8016655
21. Kara S, Li W (2011) Unit process energy consumption models for material removal processes. CIRP Ann Manuf Technol 60(1):37–40. doi:10.1016/j.cirp.2011.03.018
22. Diaz N, Redelsheimer E, Dornfeld D (2011) Energy consumption characterization and reduction strategies for milling machine tool use. Glocalized Solutions for Sustainability in Manufacturing—Proceedings of the 18th CIRP International Conference on Life Cycle Engineering. Springer Science and Business Media, LLC, pp 263–267. doi: 10.1007/978-3-642-19692-8-46
23. Li L, Yan JH, Xing ZW (2013) Energy requirements evaluation of milling machines based on thermal equilibrium and empirical modelling. J Clean Prod 52:113–121. doi:10.1016/j.jclepro.2013.02.039
24. Guo YS, Loenders J, Duflou J, Lauwers B (2012) Optimization of energy consumption and surface quality in finish turning. Procedia CIRP 1(1):512–517. doi:10.1016/j.procir.2012.04.091
25. Xie J, Liu F, Qiu H (2016) An integrated model for predicting the specific energy consumption of manufacturing processes. Int J Adv Manuf Technol 85(5–8):1339–1346
26. Jia S, Tang RZ, Lu JX (2013) Therblig-based modeling methodology for cutting power and its application in external turning. Comput Integr Manuf Syst 19(5):1015–1024